Dimerization of elongator protein 1 is essential for Elongator complex assembly

Huisha Xu[a,b,1], Zhijie Lin[a,b,1], Fengzhi Li[a,b,1], Wentao Diao[a,b,c,1], Chunming Dong[a,b], Hao Zhou[a,b], Xingqiao Xie[a,b], Zheng Wang[a,b], Yuequan Shen[a,b,d,2], and Jiafu Long[a,b,2]

[a]State Key Laboratory of Medicinal Chemical Biology, Nankai University, Tianjin 300071, China; [b]College of Life Sciences, Nankai University, Tianjin 300071, China; [c]Henan Key Laboratory of Microbial Engineering, Biology Institute of Henan Academy of Sciences, Zhengzhou 450008, China; and [d]Collaborative Innovation Center of Chemical Science and Engineering (Tianjin), Tianjin 300071, China

Edited by Yigong Shi, Tsinghua University, Beijing, China, and approved July 20, 2015 (received for review February 7, 2015)

The evolutionarily conserved Elongator complex, which is composed of six subunits elongator protein 1 (Elp1 to -6), plays vital roles in gene regulation. The molecular hallmark of familial dysautonomia (FD) is the splicing mutation of Elp1 [also known as IκB kinase complex-associated protein (IKAP)] in the nervous system that is believed to be the primary cause of the devastating symptoms of this disease. Here, we demonstrate that disease-related mutations in Elp1 affect Elongator assembly, and we have determined the structure of the C-terminal portion of human Elp1 (Elp1-CT), which is sufficient for full-length Elp1 dimerization, as well as the structure of the cognate dimerization domain of yeast Elp1 (yElp1-DD). Our study reveals that the formation of the Elp1 dimer contributes to its stability in vitro and in vivo and is required for the assembly of both the human and yeast Elongator complexes. Functional studies suggest that Elp1 dimerization is essential for yeast viability. Collectively, our results identify the evolutionarily conserved dimerization domain of Elp1 and suggest that the pathological mechanisms underlying the onset and progression of Elp1 mutation-related disease may result from impaired Elongator activities.

familial dysautonomia | Elongator complex | Elp1 subunit | dimerization | complex assembly

Familial dysautonomia (FD) (Online Mendelian Inheritance in Man: 223900), which is an Ashkenazi Jewish disorder with an incidence of 1:3,700 live births, is an autosomal recessive disorder that affects the development and survival of sensory, sympathetic, and some parasympathetic neurons (1). FD patients are characterized by cardiovascular instability, gastrointestinal dysfunction, vomiting crises, decreased sensitivity to pain and temperature, and recurrent pneumonias (2). The most common mutation, which represents >99.5% of all FD patients, is a T-to-C transition in position six of the donor splice site of intron 20 in the gene transcript of the IκB kinase (IKK) complex-associated protein (IKAP), also known as elongator protein 1 (Elp1) (3, 4). This splicing mutation causes skipping of exon 20 and results in encoding a truncated IKAP/Elp1 protein (referred to as Elp1-FD hereafter) (Fig. 1*A*).

IKAP/Elp1 was originally identified as a scaffold protein and a regulator for IKKs involved in proinflammatory cytokine signaling (5). However, contrary to this observation, subsequent analyses failed to demonstrate an association with IKKs (6). Coincident and subsequent studies supported the notion that IKAP/Elp1 is a component of the highly conserved Elongator complex from different species (7–9) (for simplicity, the term Elp1 will be used in the following discussion). The holo-Elongator complex contains six subunits (Elp1 to -6) and assembles into a core subcomplex (Elp1 to -3) and an accessory subcomplex (Elp4 to -6), which is involved in substrate recognition (10, 11). Moreover, the holo-Elongator is a functional unit, as illustrated in yeast, in which strains lacking any of the six Elp proteins exhibit similar phenotypes (7, 12, 13), and in that the removal of any Elongator subunits affects the interactions of the other subunits (14). Within the Elongator complex, Elp3 is the catalytic subunit and acetylates histones in vitro (8) and in vivo (15, 16). These findings and studies [which demonstrate the association of the Elongator complex with the RNA polymerase II (RNAPII) holoenzyme, its ability to bind to nascent pre-mRNA, and the facilitation of RNAPII transcripts through chromatin in an acetyl-CoA–dependent manner] support its role in transcriptional regulation (7, 9, 17). In addition to its participation in transcriptional regulation, the Elongator complex may also play a pivotal role in the regulation of translation through its direct effect on tRNA modification, from archaeal organisms to mammals (18–22).

Coincident with the dual roles of Elongator in transcriptional and translational regulation, it has been shown that several genes involved in cell migration and a few meiotic genes during spermatogenesis were down-regulated in FD-derived fibroblasts (23) and in mouse upon Elp1 depletion (22), respectively, and that several genes involved in oligodendrocyte development and myelin formation were down-regulated both in the cerebrum of FD patients (24) and in an FD mouse model (25). Recently, Frances Lefcort and coworkers discovered that Elp1 is essential for the genesis of tropomyosin-related kinase A nociceptors and thermoreceptors in mice (26). This role is consistent with the pain and temperature insensitivity phenotype of FD patients. Despite the paramount roles of Elp1 in controlling gene regulation, the precise mechanisms by which Elp1 functions in Elongator assembly or in the regulation of Elongator activities are poorly understood.

Here, we find that disease-related mutations in Elp1 affect Elongator assembly and have determined the atomic structures of both the C-terminal portion of human Elp1 (Elp1-CT) and the dimerization domain of Elp1 from yeast (yElp1-DD). Our results

Significance

Elongator is a highly conserved multiprotein complex composed of six subunits elongator protein 1 (Elp1 to -6). Elongator has been associated with various cellular activities and has attracted clinical attention because of its role in certain neurodegenerative diseases. To understand the mechanism of Elongator assembly, we identified the highly conserved dimerization domain in both human and yeast Elp1 subunits and solved the crystal structures of the dimerization domains. This study is a mechanistic analysis of Elp1 dimerization, which plays an essential role in the integrity of functional Elongator and suggests that the pathological mechanisms underlying the onset and progression of Elp1 mutation-related diseases may result from impaired Elongator activities.

Author contributions: H.X., Z.L., F.L., W.D., Y.S., and J.L. designed research; H.X., Z.L., F.L., W.D., C.D., H.Z., X.X., and Z.W. performed research; Y.S. contributed new reagents/analytic tools; H.X., Z.L., W.D., C.D., H.Z., Y.S., and J.L. analyzed data; and J.L. wrote the paper.

The authors declare no conflict of interest.

This article is a PNAS Direct Submission.

Data deposition: The atomic coordinates and structure factors have been deposited in the Protein Data Bank, www.pdb.org (PDB ID codes 5CQR and 5CQS).

[1]H.X., Z.L., F.L., and W.D. contributed equally to this work.

[2]To whom correspondence may be addressed. Email: long.lab@icloud.com or yuequan74@yahoo.com.

This article contains supporting information online at www.pnas.org/lookup/suppl/doi:10.1073/pnas.1502597112/-/DCSupplemental.

BIOCHEMISTRY

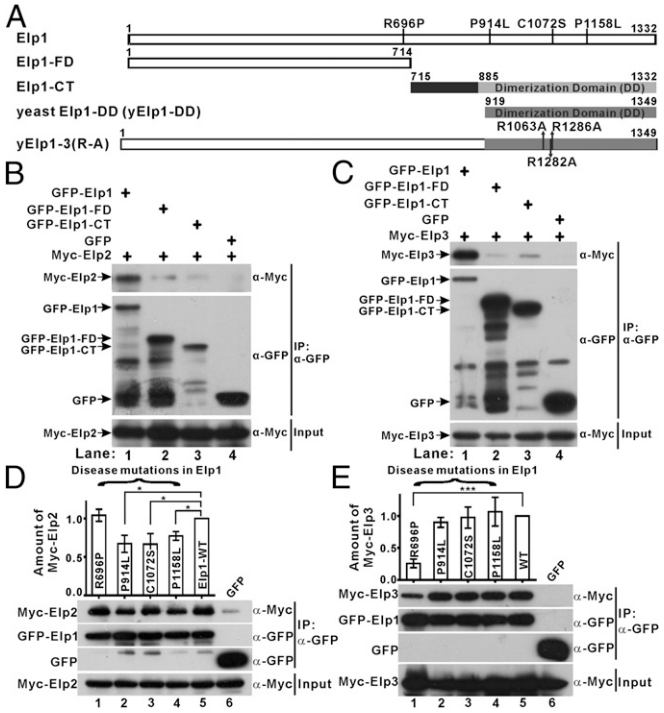

Fig. 1. Disease-related mutations in Elp1 affect its interaction with Elp2 and Elp3. (*A*) Schematic representation of full-length human Elp1 (residues 1–1332), disease-related Elp1-FD (residues 1–714), Elp1-CT (residues 715–1332), the dimerization domain of yeast Elp1 (residues 919–1349, yElp1-DD), and the yElp1 mutant. Four disease-related missense mutations in familial dysautonomia and bronchial asthma are shown in the sequence of full-length human Elp1. The dimerization domain of human Elp1 consists of residues 885–1332. The yElp1-3 (R-A) mutant was generated by substitution of residues R1063, R1282, and R1286 with alanine. (*B–E*) Coimmunoprecipitation (co-IP) experiments. The interactions between (*B*) Elp2 or (*C*) Elp3 and two Elp1 fragments and between (*D*) Elp2 or (*E*) Elp3 and Elp1 containing various disease-related mutations were evaluated using a co-IP strategy. Extracts were prepared from the transfection of HEK293T cells. Error bars indicate the standard error of the mean (SEM) ($n = 3$, separate experiments). $^{*}P < 0.05$, $^{***}P < 0.001$.

clearly reveal that the obligate dimer of Elp1 is important for both human and yeast Elongator assembly and elucidate the mechanisms responsible for human diseases caused by Elp1 mutations.

Results

The Mutated Elp1 Affects the Integrity of Elongator in Several Human Diseases. The major (>99.5%) FD-causing mutation has been identified in individuals of Ashkenazi Jewish descent (3, 4). This mutation alters the *Elp1* transcript splicing process and results in the production of a truncated form of Elp1 (residues 1–714, Elp1-FD) (Fig. 1*A*). This observation, together with the notion that Elp1 is a scaffold protein that is essential for the assembly of a functional Elongator (14), indicates that the disease-related Elp1-FD may lose its ability to bind the elongator protein 2 (Elp2) and elongator protein 3 (Elp3) subunits. To evaluate this hypothesis, we used a coprecipitation strategy in HEK293T cells. Notably, WT human GFP-Elp1 specifically coprecipitated with Myc-Elp2 (lane 1 in Fig. 1*B*) and Myc-Elp3 (lane 1 in Fig. 1*C*) whereas the disease-related GFP-Elp1-FD coprecipitated negligible amounts of both Myc-Elp2 and Myc-Elp3 (lane 2 in Fig. 1 *B* and *C*, respectively). This result may correlate with the observation that expression of Elp1-FD results in a nonfunctional protein in mouse leading to developmental delay and cardiovascular and brain malformations accompanied with early embryonic lethality (27). Interestingly, the C-terminal portion of Elp1 (residues 715–1332, Elp1-CT) (Fig. 1*A*) also lost the ability to bind both Myc-Elp2 and Myc-Elp3 (lane 3 in Fig. 1 *B* and *C*, respectively). These results indicate that full-length Elp1 is necessary for the assembly of the core Elp1-3 subcomplex, which is disrupted in FD patients and thus results in the loss of Elongator transcriptional and translational regulation of gene expression.

In addition to the major FD-causing mutation in Elp1, a second minor missense (R696P) mutation has been identified in the Ashkenazi Jewish population (3, 4), and a second missense (P914L) mutation has been identified in patients of non-Jewish descent (28) (Fig. 1*A*). Additionally, it has been reported that two amino acid substitutions (C1072S and P1158L) in Elp1 significantly increase the risk for early-onset bronchial asthma (BA), which is one of the most common inflammatory diseases worldwide (29) (Fig. 1*A*). Next, we evaluated the binding affinities between GFP-Elp1 containing these disease-related point mutations and Myc-Elp2 or Myc-Elp3. Interestingly, among these mutations in Elp1, the R696P mutant binds to Elp2 (lane 1 compared with lane 5 in Fig. 1*D*) and Elp3 (lane 1 compared with lane 5 in Fig. 1*E*) with similar and ∼70% decreased affinities, respectively. Mutations of P914, C1072, and P1158 result in ∼23–33% decreased affinities for Elp2 (lanes 2–4 compared with lane 5 in Fig. 1*D*) whereas mutations of these residues do not affect the binding to Elp3 (lanes 2–4 compared lane 5 in Fig. 1*E*). Nevertheless, these results clearly indicate that the disease-related point mutations in Elp1 affect the integrity of Elongator, which may be partially associated with mechanisms responsible for FD or BA.

Overall Structure of the C-Terminal Portion of Human Elp1. The C-terminal portion of Elp1 (residues 715–1332, Elp1-CT), which is absent from Elp1-FD in FD and which contains most of the amino acid substitutions in FD or BA, is important for Elongator assembly (Fig. 1). To elucidate the molecular mechanism governing Elp1-mediated Elongator assembly, we determined the crystal structure of the human Elp1-CT using single anomalous dispersion at a resolution of 3.0 Å (Table S1). The crystal belongs to the space group $P6_122$ and contains one Elp1-CT molecule per asymmetric unit. The overall structure of Elp1-CT is composed of 28 α-helices, forming a "C"-shaped architecture (Fig. 2*A*). The waist of the C contains six double-helix repeats (α15–26) that exhibit structural similarity to tetratrico-peptide repeats (TPRs) (Fig. S1*A*) and is referred to as the TPR-like domain (Fig. 2*A*). Helices α27 and α28 form a three-helix bundle with the elongated α26, which together cap the C-terminal TPR-like domain. The extreme C terminus of Elp1-CT exhibits extensive hydrophobic interactions with α27/28 via residues W1326, L1328, L1330, and L1331 (Fig. 2 *A*, *A1*). N-terminal to the TPR-like domain, helices α1 to -14 form an elongated α-solenoid domain whose axis is nearly perpendicular to the TPR-like domain. α14 functions as a kink to maintain the TPR-like domain and α-solenoid domain at nearly a 90° angle. On one hand, α14 caps the TPR-like domain with the hydrophobic residue F934, which packs against a hydrophobic surface formed by A946, L950, and L964 of α15/16 (Fig. 2 *A*, *A2*). On the other hand, α14 uses I936 and L940 to stack against the hydrophobic surface formed by L895, Y898, and F900 of α11/12. These residues at the interface between α14 and the TPR-like or α-solenoid domain are highly conserved from yeast to humans (Fig. S2), which together contribute to the formation of the C-shaped scaffold of Elp1-CT. Using the Dali server, we did not identify a structure in the Protein Data Bank that shares a similar fold as Elp1-CT. Thus, these structural analyses indicated that Elp1-CT may assemble into a novel and evolutionarily conserved C-shaped structure.

Elp1-CT Is a Homodimer in Solution and Forms a Horseshoe-Shaped Structure. To evaluate its conformation in solution, Elp1-CT was purified to homogeneity (Fig. S3*A*) and analyzed using analytical ultracentrifugation. Sedimentation velocity (SV) analysis indicated that Elp1-CT forms a stable homodimer (black line in Fig. 2*B*). Sedimentation equilibrium (SE) analysis further confirmed that

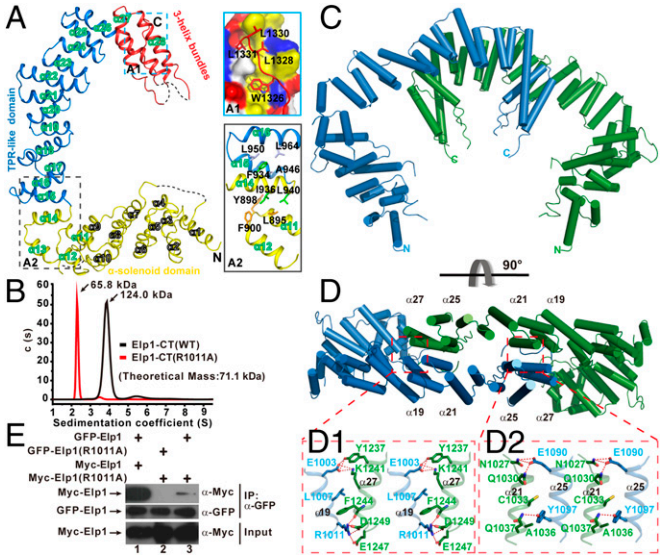

Fig. 2. The horseshoe-shaped structure of the Elp1-CT homodimer, which is required for full-length Elp1 self-association. (*A*) Ribbon representation of the overall structure of Elp1-CT. The α-solenoid domain (yellow), TPR-like domain (blue), and three-helix bundle (red) are shown. (*A1*) The C-tail packs against a hydrophobic surface, with negatively charged, positively charged, and hydrophobic residues colored red, blue, and yellow, respectively. (*A2*) α14 participates in hydrophobic interactions with α11/12 and α15/16. The missing loops (residues 801–810, 912–914, 1132–1224, and 1270–1320) are shown as dashed lines. The α-helices in the dimerization domain of Elp1-CT are labeled in green. The N and C termini of the protein are labeled. (*B*) The c(S) distribution from SV analysis of Elp1-CT (black line) and Elp1-CT(R1101A) (red line). (*C*) Schematic representation of the homodimer of Elp1-CT. The two molecules are colored blue and green. (*D*) Stereoviews of the interactions of the Elp1-CT homodimer. One of two identical interfaces is formed (*D1*) between α19 of the blue monomer and α27 of the green monomer and (*D2*) between α21 of the blue monomer and α25 of the green monomer. (*E*) The full-length Elp1 self-associates in vivo via Elp1-CT dimerization. Extracts were prepared from the transfection of HEK293T cells.

Elp1-CT assembles into a homodimer with a molecular mass of ∼137.97 kDa (Fig. S4 *A*–*C*).

With a crystallographic twofold axis, the overall shape of the Elp1-CT homodimer resembles a horseshoe-shaped structure (Fig. 2*C*). The helices α19 and α21 of one molecule participate in several polar and hydrophobic interactions with α27 and α25 of the second molecule, respectively (Fig. 2*D*). In detail, E1003 and R1011 of α19 form salt bridges with K1241 and E1247/D1249 of α27, respectively (Fig. 2 *D*, *D1*). E1003 and R1011 also form hydrogen bonds with the side chain of Y1237 and main chain of F1244, respectively. α27 also participates in hydrophobic interactions with α19 via the side chains of L1007, R1011, and F1244. α21 and α25 primarily interact via hydrogen bonds contributed by residues N1027, Q1030, Q1037, E1090, and Y1097. More detailed interactions are shown in Fig. 2 *D*, *D2*. Next, we directly evaluated the role of the interactions between the monomers in the homodimer. To this end, the residue R1011, which is conserved from fly to human (Fig. S2), was mutated to alanine in Elp1-CT [referred to as Elp1-CT(R1011A)]. Consistent with the structure-based prediction, mutation of R1011 to alanine disrupted Elp1-CT dimer assembly. The purified Elp1-CT(R1011A) exists as a monomer in solution with a molecular mass of ∼65.8 kDa according to SV analysis (Fig. S3*A* and red line in Fig. 2*B*). Circular dichroism confirmed a similar overall secondary structure for WT and mutant Elp1-CT, which indicated that the conformational changes were not due to protein folding (Fig. S3*B*). Collectively, we conclude that Elp1-CT, which is absent from Elp1-FD in FD patients, forms a horseshoe-shaped dimer structure in solution.

The Dimerization Domain in Elp1-CT Is Sufficient for Full-Length Elp1 Self-Association in Vivo. To investigate Elp1-CT–mediated self-association of the full-length Elp1 in vivo, we used a coprecipitation strategy using two different tags on Elp1 and evaluated their interaction in the context of either the WT Elp1 or the mutant Elp1 (R1011A). As expected, WT GFP-Elp1 specifically coprecipitated with Myc-Elp1 (lane 1 in Fig. 2*E*) whereas the mutant GFP-Elp1 (R1011A) did not form a complex with the mutant Myc-Elp1 (R1011A) (lane 2 in Fig. 2*E*). Interestingly, negligible amounts of the mutant Myc-Elp1(R1011A) coprecipitated with WT GFP-Elp1, indicating that Elp1 may assemble into a very stable dimer in vivo and correlated with the buried surface area of 1,732 Å^2 for Elp1-CT dimer calculated using PISA (30). Importantly, in another coprecipitation assay, GFP-Elp1-CT coprecipitated a similar amount of Myc-Elp1 as full-length GFP-Elp1 (lane 2 compared with lane 3 in Fig. S4*D*) whereas GFP-Elp1-FD did not form a complex with Myc-Elp1 (lane 1 in Fig. S4*D*), indicating that Elp1-CT contains a dimerization domain that is sufficient for Elp1 self-association. Moreover, we further mapped the dimerization domain of Elp1 to residues 885–1332 (Fig. S4*E* and Fig. 1*A*). Collectively, our results indicate that the dimerization domain is sufficient for full-length Elp1 self-association in vivo.

Attempts to purify the recombinant full-length human Elp1 were unsuccessful; therefore, it was not possible to evaluate whether Elp1 assembles into a homodimer in vitro. Nevertheless, the yeast ortholog of Elp1 assembles into a homodimer via its cognate dimerization domain; therefore, it can be assumed that human Elp1 is able to form a homodimer to create a platform to dock various factors during complex formation (e.g., Elongator complex assembly) (discussed in detail in *Elp1 Self-Association Contributes to its Stability and Is Important for Elongator Assembly* and *yElp1 Dimerization Is Important for Yeast Elongator Assembly and Yeast Cell Viability*).

Overall Structure of the Dimerization Domain of Yeast Elp1. Cross-species complementation studies (21, 31) indicate that the structural features of each Elongator subunit are highly conserved among all eukaryotes. To evaluate this speculation, we investigated the structural features of Elp1 from *Saccharomyces cerevisiae* because Elongator was initially identified in this species (7). Accordingly, we purified yeast Elp1 (referred to as yElp1, using a similar nomenclature for each yeast Elongator subunit hereafter) to homogeneity (*Inset* in Fig. 3*A*). The SV analysis indicated that yElp1 assembles into a homodimer with a molecular mass of ∼316 kDa (black line in Fig. 3*A*). To understand the molecular mechanism of yElp1 dimerization, we attempted to determine the crystal structure of yElp1; however, these experiments were unsuccessful. According to secondary structure prediction and sequence alignment with the dimerization domain of human Elp1, we identified the cognate dimerization domain of yElp1 (referred to as yElp1-DD hereafter) as residues 919–1349 (Fig. 1*A* and Fig. S2) and subsequently successfully obtained crystals of yElp1-DD.

The crystal structure of yElp1-DD was determined at a resolution of 2.7 Å, with four molecules in the asymmetric unit (Table S1). These four molecules adopt an identical conformation, with a core root-mean-square deviation (rmsd) of 0.54–0.75 Å, and form two head-to-head dimers (rmsd value of 0.88 Å) in the crystal (Fig. S1*B*). Superimposition of the structures of the yElp1-DD and Elp1-CT homodimers resulted in an rmsd of 2.6 Å for 518 equivalent Cα atoms (Fig. S1*C*), indicating that human and yeast Elp1 share a similar dimeric structure. Notably, the sequence identity is low between the yeast and human Elp1 dimerization domains (Fig. S2); thus, the residues at each dimer interface are divergent (Figs. 2*D* and 3*C*). There are two primary packing surfaces in the dimer interface of yElp1-DD, with a total buried surface area of 2,045 Å^2. First, α7'-11' of one molecule interacts with α16'-18' via several polar and hydrophobic interactions (Fig. 3 *C*, *C1*). In particular, R1015, E1046, and R1063 of one molecule form salt bridges with E1287, R1282, and E1278 of

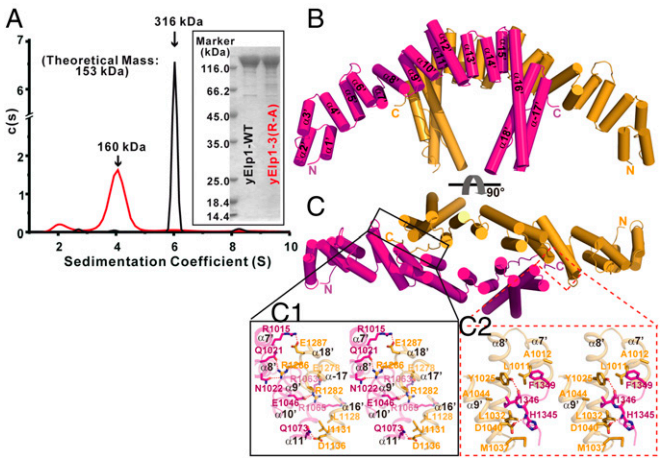

Fig. 3. Structure of the yeast Elp1 dimerization domain (yElp1-DD). (*A*) The c(S) distribution from SV analysis of yElp1-WT (black line) and the mutant yElp1-3(R-A) (red line). (*Inset*) The 15% SDS/PAGE analysis of the purified proteins. (*B*) Schematic representation of the homodimer of the dimerization domain of yeast Elp1 (residues 919–1349, yElp1-DD). The two monomers are colored magenta and gold. The N and C termini of each monomer are labeled. (*C*) Stereoviews of the interactions of the yElp1-DD homodimer. One of two identical interfaces is formed (*C1*) between helices (α7′-11′) of the magenta monomer and helices (α16′-18′) of the gold monomer and (*C2*) between residues of the extreme C terminus of the magenta monomer and helices (α7′-9′) of the gold monomer.

the other molecule, respectively. Residues Q1021/N1022/R1065/Q1073 and R1286/L1128/I1131/D1036 form hydrogen bonds and participate in hydrophobic interactions at the dimer interface between the two molecules. The second packing surface is the interface between helices α7′-9′ and the extreme C-tail of the two molecules (Fig. 3 *C*, *C2*). The C-tail primarily uses the hydrophobic residues I1346 and F1349 to pack against the hydrophobic surface (formed by L1011, A1012, Y1025, L1032, M1037, and A1044) of α7′-9′.

Next, we investigated the yElp1-DD–mediated dimerization of full-length yElp1 in solution by mutating residues within the interface of the yElp1-DD homodimer. To this end, a mutant was designed to disrupt the yElp1-DD homodimer by substituting residues R1063, R1282, and R1286 with alanines [referred to as yElp1-3(R-A) hereafter] (Fig. 1*A*). The mutant yElp1-3(R-A) was purified to homogeneity (*Inset* in Fig. 3*A*) and analyzed by SV analysis. Consistent with the structure-based prediction, the purified yElp1-3(R-A) exists as a monomer in solution with a molecule mass of ∼160 kDa according to SV analysis (red line in Fig. 3*A*). Collectively, these structural and biochemical results indicate that yElp1 assembles into a homodimer via yElp1-DD–mediated dimerization, thereby providing a rationale for a previous finding that a tagged yElp1 (yElp1-CBP) was able to coprecipitate a second yElp1 carrying a different tag (yElp1-ProtA) and further updating a proposed model of Elongator assembly (11).

Elp1 Self-Association Contributes to Its Stability and Is Important for Elongator Assembly. Elp1 is considered to primarily function not only as a scaffold required for the formation of Elongator, and therefore confers stability to the overall complex (14), but also as a docking site for various factors that regulate Elongator activity (summarized in ref. 32). These findings, as well as our results demonstrating the conserved dimeric assembly of both human and yeast Elp1 and the notion that Elp1 is mutated in several diseases, indicate that the dimerization domain-mediated Elp1 self-association may be important for Elongator function. To evaluate this hypothesis, we used several approaches. First, we demonstrated that the Elp1-CT homodimer is much more stable than the mutant Elp1-CT(R1011A) monomer (Fig. S5*A*). Next, we evaluated the stability of full-length Elp1 in HeLa cells. Accordingly, the endogenous Elp1 protein was knocked down by shRNA (Fig. S5*B*). Subsequently, either the exogenous shRNA-resistant GFP-Elp1 or GFP-Elp1(R1011A) (which is incapable of self-association) fusion protein was overexpressed in Elp1-depleted HeLa cells. Notably, although the mRNA level of the exogenous mutant Elp1(R1011A) was similar to that of the WT Elp1 (Fig. S5*C*), the protein level of the mutant Elp1(R1011A) decreased to ∼30% of that of WT Elp1 (Figs. S5 *D* and *E*). To further evaluate the role of Elp1 dimerization on its stability, we used a cycloheximide (CHX) chase assay. We blocked de novo protein synthesis with CHX in Elp1-depleted HeLa cells overexpressing shRNA-resistant GFP-Elp1 or GFP-Elp1(R1011A) and analyzed the protein levels by immunoblotting. As determined by the CHX chase assay, the half-life of WT Elp1 was longer than that of the Elp1(R1011A) mutant (Figs. S5 *F* and *G*). Together, these results indicate that Elp1 self-association may contribute to its stability in vivo.

Elp1 has been shown to bind strongly to Elp2 and Elp3; this Elp1-3 subcomplex is stable in high salt concentrations (12). We used a coprecipitation strategy to evaluate the role of Elp1 self-association in the assembly the Elp1-3 subcomplex. As expected, GFP-Elp1 specifically coprecipitated with Myc-Elp2 and Myc-Elp3 to form a tripartite Elp1-3 subcomplex (lane 1 in Fig. 4*A*). Notably, significantly decreased amounts of both Myc-Elp2 and Myc-Elp3 coprecipitated with the mutant GFP-Elp1(R1011A), indicating that the Elp1-3 subcomplex is less stable in the context of the Elp1 self-association–deficient mutant. Next, we showed that Elp1 self-association is required for the binding between the core Elp1-3 complex and the accessory Elp4-6 subcomplexes (Fig. 4*B*) or for assembling the holo-Elongator complex (Fig. S6*A*) via similar coimmunoprecipitation strategies. Collectively, these results indicate that Elp1 self-association not only contributes to its stability but also is essential for conferring stability to the human holo-Elongator complex.

yElp1 Dimerization Is Important for Yeast Elongator Assembly and Yeast Cell Viability. The above results indicate that Elp1 self-association contributes to its stability and that Elongator formation is dependent on full-length Elp1 as well as the composite surface of the Elp1 dimer. We next investigated whether dimerization-mediated yElp1 self-association contributes to its stability and is essential for the formation of yeast Elongator. Accordingly, we showed that disruption of self-association decreased the stability of yElp1 using a trypsin digestion assay (Fig. S5*H*). We next tested yeast Elongator assembly in the context of either WT

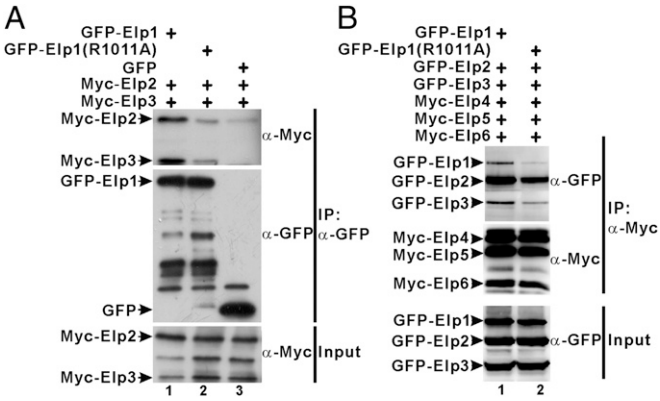

Fig. 4. Elp1 self-association is important for holo-Elongator assembly. Co-IP experiments of (*A*) the core subcomplex formation by Elp1 and (*B*) the binding between the core Elp1-3 and the accessory Elp4-6 subcomplexes. Extracts were prepared from the transfection of HEK293T cells.

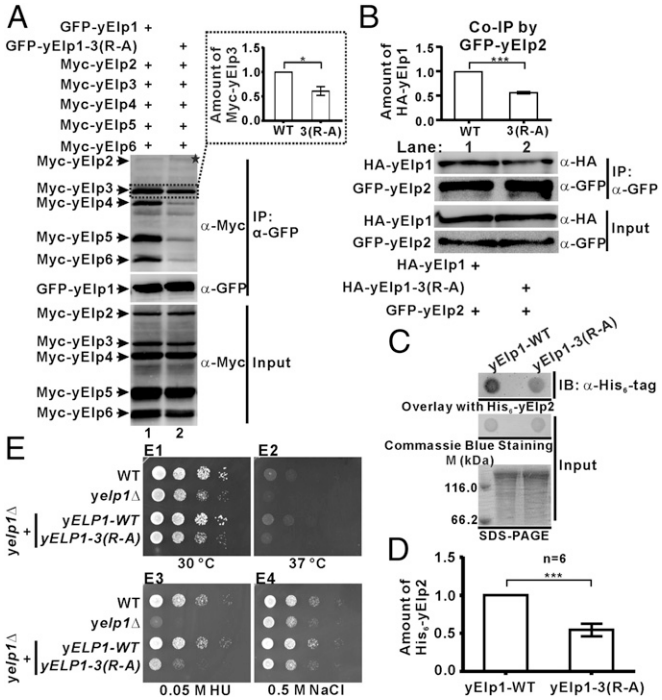

Fig. 5. Yeast Elp1 (yElp1) self-association is essential for the integrity of a functional yeast Elongator. (*A*) Co-IP experiments for yeast holo-Elongator complex formation by yElp1 self-association. Extracts were prepared from the transfection of HEK293T cells. The nonspecific faint band is marked with a star in the *Upper* panel. (*B*) Co-IP experiments of the interaction between yElp1 WT or its mutant and yElp2. Extracts were prepared from yeast cells after homologous recombination as indicated in *SI Materials and Methods*. The error bars in *A* and *B* indicate the SEM ($n = 3$). $^{*}P < 0.05$. $^{***}P < 0.001$. (*C*) Dot-blot overlay assay of WT yElp1 or its mutant and yElp2. Bound yElp2 was detected by immunoblotting with an antibody against the His_6-tag (*Top*). The PVDF membrane was stained with Coomassie blue (*Middle*). WT yElp1 and its mutant were resolved by SDS/PAGE to normalize the sample inputs (*Bottom*). (*D*) Bar graph of yElp2 binding. The error bar indicates the SEM ($n = 6$). $^{***}P < 0.001$. (*E*) yElp1 self-association is essential for yeast cell viability. Strains of the indicated genotype were grown to late log phase/stationary phase (overnight) and plated in serial dilutions on a yeast peptone dextrose (YPD) plate. The plates are shown after 40 h of incubation at (*E1*) 30 °C, at (*E2*) 37 °C, on (*E3*) YPD containing 50 mM hydroxyurea (HU), and on (*E4*) YPD containing 0.5 M NaCl.

HA-yElp1 or the mutant HA-yElp1-3(R-A) using coprecipitation assays. As expected, HA-yElp1 specifically coprecipitated with Myc-tagged yElp3-6 subunits in HEK293 cells (lane 1 in Fig. 5*A*). Notably, negligible amounts of the yElp4-6 subcomplex and significantly decreased amounts of yElp3 coprecipitated with the mutant HA-yElp1-3(R-A) (lane 2 in Fig. 5*A*). Interestingly, Myc-yElp2 did not coprecipitate with GPF-yElp1 in extracts prepared from HEK293 cells (lane 1 in Fig. 5*A*). However, GFP-yElp2 did coprecipitate with HA-yElp1 in the extracts prepared from yeast cells (lane 1 in Fig. 5*B*). Decreased levels of the mutant HA-yElp1-3(R-A) coprecipitated with either GFP-yElp2 (Fig. 5*B*) or Myc-yElp3 (Fig. S6*B*) in the extracts prepared from yeast cells compared with WT HA-Elp1. We also showed that the purified monomeric mutant yElp1-3(R-A) bound to the purified yElp2 with ∼50% decreased affinity compared with purified yElp1-WT (Fig. 5 *C* and *D*). Together, these results indicate that yElp1 self-association is also important for yeast Elongator formation.

The previously described structural and biochemical results clearly demonstrated that the conserved Elp1 self-association is important for the assembly of human and yeast Elongator. Next, we used yeast as a host to investigate the role of yElp1 in vivo. To this end, a *yelp1Δ* strain was generated by replacing the y*ELP1* gene with *S. cerevisiae URA3* (Table S2). As expected, yeast cells with *yelp1Δ* exhibited typical *elp* phenotypes [e.g., the slow-start phenotype and sensitivity to temperature, hydroxyurea (HU), and salt] (Fig. 5*E*), which is consistent with previous studies (7, 12, 13). To further explore the role of yElp1 in vivo, we evaluated the importance of yElp1 self-association–mediated Elongator assembly using a complementation assay. To evaluate their ability to complement *elp* phenotypes, the plasmids pP1K-3HA-yElp1(404) and pP1K-3HA-yElp1-3(R-A) and the corresponding empty vectors were linearized and integrated into the *yelp1Δ* strain. Interestingly, expression of the WT y*ELP1* (y*ELP1*-WT), but not of the mutant y*ELP1-3(R-A)*, could fully rescue the *yelp1Δ* phenotype (Fig. 5*E*). Collectively, these results indicate that Elp1 self-association–mediated Elongator assembly is crucial for yeast growth.

Discussion

The crystal structures of human and yeast Elp1 presented in this study provide for the first time, to our knowledge, structural insights into the roles of Elp1 in Elongator assembly and activities. Our analysis reveals that the C terminus of both human and yeast Elp1 contains an evolutionarily conserved dimerization domain. These dimerization domains, which are sufficient for full-length protein self-association and are necessary for Elongator assembly, assemble into novel structures composed of tandem repeats of an α-helical structural unit (Figs. 2 and 3) with a very similar dimeric conformation although the sequence identity is low between human and yeast Elp1 (Fig. S2). Therefore, it can be assumed that the structural and biochemical features of the Elp1 dimerization domain described herein are shared by the orthologs of Elp1 in other eukaryotic species.

A recent study indicated that the yElp2 subunit is a monomer in solution (16). Consistent with this observation, negligible amounts of Myc-yElp2 coprecipitated with GFP-yElp2 in the extracts prepared from a *yelp1* knockout yeast strain (lane 3 in Fig. S6*C*). Notably, Myc-yElp2 specifically coprecipitated with GFP-yElp2 in the presence of WT yElp1 whereas the amounts of Myc-yElp2 that coprecipitated with GFP-yElp2 were markedly decreased with the self-association deficient mutant yElp1-3 (R-A) (lane 2 compared with lane 1 in Fig. S6*C*), indicating that the yElp1 dimer is required for recruiting two copies of yElp2 for yElp1-mediated complex (e.g., yeast holo-Elongator) formation. Using a similar coimmunoprecipitation strategy, we showed that both the yeast and human Elp1 dimers are also required for incorporating two copies of yElp3 (Fig. S6*D*) or human Elp3 (Fig. S6*E*), respectively, into Elp1-mediated complexes.

A previous study had demonstrated that yElp1 binds to tRNA with its basic region (33). We next tested the role of Elp1 self-association in its tRNA-binding ability using an electrophoretic mobility shift assay. The acquired data clearly indicated that the monomeric mutants of both human Elp1-CT (Fig. S7*A*) and yeast full-length Elp1 (Fig. S7*B*) have comparable binding affinities for their cognate tRNA targets (e.g., $tRNA_{Glu}^{UUC}$, a substrate of Elongator) compared with the WT proteins, indicating that Elp1 self-association is dispensable for tRNA binding, at least for $tRNA_{Glu}^{UUC}$.

Several previous studies have indicated that overexpression of the N-terminal half of Elp1 could neither rescue Elp1 depletion-caused defects in adhesion and migration in several cell types (34) nor rescue early embryonic lethality induced by a complete loss of Elp1 in mouse (27, 35). One explanation may be that the C-terminal dimerization domain of Elp1 (identified in this study) is obligatory for its normal function, at least for Elongator assembly.

Based on the observation of Elp1 that dimerization is essential for Elongator assembly (Fig. 4), we can conclude that the function of Elongator may be impaired as a consequence of the self-association deficiency of Elp1 in most FD patients (>99.5% of FD cases) (Fig. 1). According to the importance of the conserved Elp1 self-association for Elp1 function, we hypothesized that

the other disease-related point mutations identified in FD and BA may disrupt Elp1 self-association. Unexpectedly, analysis of the crystal structure of Elp1-CT revealed that the residues P914, C1072, and P1158, which are mutated in Elp1 of FD and BA patients, lie far from the dimer interface of Elp1-CT (Fig. S8*A*). Consistent with this structural observation, GFP-Elp1 containing P914L, C1072S, or P1158L coprecipitated with Myc-Elp1 (Fig. S8*B*), indicating that these disease-related mutations do not affect Elp1 self-association. Notably, mutation of R696 to proline, which is another FD-related mutation, also did not alter the state of Elp1 self-association (Fig. S8*B*) because this residue lies outside of the Elp1 dimerization domain (Fig. 1*A*). Nevertheless, these four disease-related mutations indeed are likely to destabilize the structural integrity of Elongator because these four point mutations affected Elp1-3 subcomplex formation to a certain extent (Fig. 1 *D* and *E*). Thus, these disease-related mutations may affect the integrity of a functional Elongator, which affects gene regulation in the progress of these diseases. Future studies are necessary to evaluate this hypothesis.

Materials and Methods

All of the proteins used in this study were expressed in BL21(DE3) Codon Plus *Escherichia coli* cells and purified by affinity chromatography followed by size-exclusion chromatography. Crystals were obtained by the sitting drop vapor diffusion method. An extended section describing protein preparation, crystallization, structure determination, yeast strain construction, and in vivo and in vitro biochemical assays can be found in *SI Materials and Methods*.

ACKNOWLEDGMENTS. We thank the staff at the beamline BL17U1 of the Shanghai Synchrotron Radiation Facility and the staff at the beamline NW3A at Photon Factory (Tsukuba, Japan) for excellent technical assistance during data collection. This work was supported by 973 Program Grants 2014CB910201 (to J.L.) and 2012CB917201 and 2013CB910400 (to Y.S.) and National Natural Science Foundation of China Grants 31270815 and 31470755 (to J.L.) and 31370826 (to Y.S.).

1. Maayan C, Kaplan E, Shachar S, Peleg O, Godfrey S (1987) Incidence of familial dysautonomia in Israel 1977-1981. *Clin Genet* 32(2):106–108.
2. Axelrod FB, Goldstein DS, Holmes C, Berlin D, Kopin IJ (1996) Pattern of plasma levels of catecholamines in familial dysautonomia. *Clin Auton Res* 6(4):205–209.
3. Anderson SL, et al. (2001) Familial dysautonomia is caused by mutations of the IKAP gene. *Am J Hum Genet* 68(3):753–758.
4. Slaugenhaupt SA, et al. (2001) Tissue-specific expression of a splicing mutation in the IKBKAP gene causes familial dysautonomia. *Am J Hum Genet* 68(3):598–605.
5. Cohen L, Henzel WJ, Baeuerle PA (1998) IKAP is a scaffold protein of the IkappaB kinase complex. *Nature* 395(6699):292–296.
6. Krappmann D, et al. (2000) The I kappa B kinase (IKK) complex is tripartite and contains IKK gamma but not IKAP as a regular component. *J Biol Chem* 275(38): 29779–29787.
7. Otero G, et al. (1999) Elongator, a multisubunit component of a novel RNA polymerase II holoenzyme for transcriptional elongation. *Mol Cell* 3(1):109–118.
8. Hawkes NA, et al. (2002) Purification and characterization of the human elongator complex. *J Biol Chem* 277(4):3047–3052.
9. Kim JH, Lane WS, Reinberg D (2002) Human Elongator facilitates RNA polymerase II transcription through chromatin. *Proc Natl Acad Sci USA* 99(3):1241–1246.
10. Lin Z, et al. (2012) Crystal structure of elongator subcomplex Elp4-6. *J Biol Chem* 287(25):21501–21508.
11. Glatt S, et al. (2012) The Elongator subcomplex Elp456 is a hexameric RecA-like ATPase. *Nat Struct Mol Biol* 19(3):314–320.
12. Winkler GS, et al. (2001) RNA polymerase II elongator holoenzyme is composed of two discrete subcomplexes. *J Biol Chem* 276(35):32743–32749.
13. Krogan NJ, Greenblatt JF (2001) Characterization of a six-subunit holo-elongator complex required for the regulated expression of a group of genes in Saccharomyces cerevisiae. *Mol Cell Biol* 21(23):8203–8212.
14. Frohloff F, Jablonowski D, Fichtner L, Schaffrath R (2003) Subunit communications crucial for the functional integrity of the yeast RNA polymerase II elongator (gamma-toxin target (TOT)) complex. *J Biol Chem* 278(2):956–961.
15. Wittschieben BØ, Fellows J, Du W, Stillman DJ, Svejstrup JQ (2000) Overlapping roles for the histone acetyltransferase activities of SAGA and elongator in vivo. *EMBO J* 19(12):3060–3068.
16. Dong C, et al. (2015) The elp2 subunit is essential for elongator complex assembly and functional regulation. *Structure* 23(6):1078–1086.
17. Gilbert C, Kristjuhan A, Winkler GS, Svejstrup JQ (2004) Elongator interactions with nascent mRNA revealed by RNA immunoprecipitation. *Mol Cell* 14(4):457–464.
18. Selvadurai K, Wang P, Seimetz J, Huang RH (2014) Archaeal Elp3 catalyzes tRNA wobble uridine modification at C5 via a radical mechanism. *Nat Chem Biol* 10(10): 810–812.
19. Huang B, Johansson MJ, Byström AS (2005) An early step in wobble uridine tRNA modification requires the Elongator complex. *RNA* 11(4):424–436.
20. Chen C, Tuck S, Byström AS (2009) Defects in tRNA modification associated with neurological and developmental dysfunctions in Caenorhabditis elegans elongator mutants. *PLoS Genet* 5(7):e1000561.
21. Mehlgarten C, et al. (2010) Elongator function in tRNA wobble uridine modification is conserved between yeast and plants. *Mol Microbiol* 76(5):1082–1094.
22. Lin FJ, Shen L, Jang CW, Falnes PO, Zhang Y (2013) Ikbkap/Elp1 deficiency causes male infertility by disrupting meiotic progression. *PLoS Genet* 9(5):e1003516.
23. Close P, et al. (2006) Transcription impairment and cell migration defects in elongator-depleted cells: Implication for familial dysautonomia. *Mol Cell* 22(4):521–531.
24. Cheishvili D, Maayan C, Smith Y, Ast G, Razin A (2007) IKAP/hELP1 deficiency in the cerebrum of familial dysautonomia patients results in down regulation of genes involved in oligodendrocyte differentiation and in myelination. *Hum Mol Genet* 16(17): 2097–2104.
25. Cheishvili D, et al. (2014) IKAP deficiency in an FD mouse model and in oligodendrocyte precursor cells results in downregulation of genes involved in oligodendrocyte differentiation and myelin formation. *PLoS One* 9(4):e94612.
26. George L, et al. (2013) Familial dysautonomia model reveals Ikbkap deletion causes apoptosis of Pax3+ progenitors and peripheral neurons. *Proc Natl Acad Sci USA* 110(46):18698–18703.
27. Dietrich P, Yue J, E S, Dragatsis I (2011) Deletion of exon 20 of the Familial Dysautonomia gene Ikbkap in mice causes developmental delay, cardiovascular defects, and early embryonic lethality. *PLoS One* 6(10):e27015.
28. Leyne M, et al. (2003) Identification of the first non-Jewish mutation in familial Dysautonomia. *Am J Med Genet A* 118A(4):305–308.
29. Takeoka S, et al. (2001) Amino-acid substitutions in the IKAP gene product significantly increase risk for bronchial asthma in children. *J Hum Genet* 46(2):57–63.
30. Krissinel E, Henrick K (2007) Inference of macromolecular assemblies from crystalline state. *J Mol Biol* 372(3):774–797.
31. Li F, Lu J, Han Q, Zhang G, Huang B (2005) The Elp3 subunit of human Elongator complex is functionally similar to its counterpart in yeast. *Mol Genet Genomics* 273(3): 264–272.
32. Glatt S, Müller CW (2013) Structural insights into Elongator function. *Curr Opin Struct Biol* 23(2):235–242.
33. Di Santo R, Bandau S, Stark MJR (2014) A conserved and essential basic region mediates tRNA binding to the Elp1 subunit of the Saccharomyces cerevisiae Elongator complex. *Mol Microbiol* 92(6):1227–1242.
34. Johansen LD, et al. (2008) IKAP localizes to membrane ruffles with filamin A and regulates actin cytoskeleton organization and cell migration. *J Cell Sci* 121(Pt 6): 854–864.
35. Chen YT, et al. (2009) Loss of mouse Ikbkap, a subunit of elongator, leads to transcriptional deficits and embryonic lethality that can be rescued by human IKBKAP. *Mol Cell Biol* 29(3):736–744.
36. Otwinowski Z, Minor W (1997) Processing of X-ray diffraction data collected in oscillation mode. *Methods Enzymol* 276:307–326.
37. Adams PD, et al. (2010) PHENIX: A comprehensive Python-based system for macromolecular structure solution. *Acta Crystallogr D Biol Crystallogr* 66(Pt 2):213–221.
38. Emsley P, Lohkamp B, Scott WG, Cowtan K (2010) Features and development of Coot. *Acta Crystallogr D Biol Crystallogr* 66(Pt 4):486–501.
39. Brünger AT, et al. (1998) Crystallography & NMR system: A new software suite for macromolecular structure determination. *Acta Crystallogr D Biol Crystallogr* 54(Pt 5): 905–921.
40. Davis IW, et al. (2007) MolProbity: All-atom contacts and structure validation for proteins and nucleic acids. *Nucleic Acids Res* 35(Web Server issue):W375–W383.
41. Schuck P (2000) Size-distribution analysis of macromolecules by sedimentation velocity ultracentrifugation and lamm equation modeling. *Biophys J* 78(3):1606–1619.
42. Schuck P (2003) On the analysis of protein self-association by sedimentation velocity analytical ultracentrifugation. *Anal Biochem* 320(1):104–124.
43. Robinson JS, Klionsky DJ, Banta LM, Emr SD (1988) Protein sorting in Saccharomyces cerevisiae: Isolation of mutants defective in the delivery and processing of multiple vacuolar hydrolases. *Mol Cell Biol* 8(11):4936–4948.